Quantum process tomography of a controlled-NOT gate

J. L. O'Brien,[1, 2, *] G. J. Pryde,[1, 2, *] A. Gilchrist,[2] D. F. V. James,[3]
N. K. Langford,[2, *] T. C. Ralph,[2] and A. G. White[2, *]

[1]*These authors contributed equally to this work.*
[2]*Centre for Quantum Computer Technology and Department of Physics,*
University of Queensland, Brisbane, Queensland 4072, AUSTRALIA
[3]*Theoretical Division T-4, University of California, Los Alamos National Laboratory,*
MS B-283, P.O. Box 1663, Los Alamos, NM 87545, USA.

We demonstrate complete characterization of a two-qubit entangling process – a linear optics controlled-NOT gate operating in the coincidence basis – by quantum process tomography. We use maximum-likelihood estimation to convert the experimental data into a physical process matrix. The process matrix allows accurate prediction of the operation of the gate for arbitrary input states, and calculation of gate performance measures such as the average gate fidelity, average purity and entangling capability of our gate, which are 0.81, 0.71 and 0.54 respectively.

Quantum information science offers the potential for major advances such as quantum computing [1] and quantum communication [2], as well as many other quantum technologies [3]. Two-qubit entangling gates, such as the controlled-NOT (CNOT), are fundamental elements in the archetypal quantum computer [1]; indeed arbitrary one-qubit rotations and *any* two-qubit, unitary, entangling gate form a universal set for quantum computation [4]. A promising proposal for achieving scalable quantum computing is that of Knill, Laflamme and Milburn (KLM), in which linear optics and measurement-induced Kerr-like nonlinearity can be used to construct CNOT gates [5]. The nonlinearity upon which the KLM and related [6, 7] CNOT schemes are built can also be used for other important quantum informatic tasks, such as quantum nondemolition measurements [8, 9] and preparation of novel quantum states (for example, [10]). An essential step in realizing such advances is the complete characterization of quantum processes.

To create a working quantum circuit, it is necessary to understand the action of each of the components, or gates, in terms of a mapping between states of the quantum system at the input and output of a gate. This *quantum transfer function* contains all possible information about the action of the gate on the input system, making the measurement and understanding of a gate's transfer function not only necessary, but also sufficient, for characterization of a quantum circuit in the input/output state space. In discrete-variable quantum information, the quantum transfer function of a gate can be represented as a *state* transfer function, expressed in terms of a *process matrix* χ. The process matrix gives the coefficients of operators acting upon the quantum state of the input qubits to generate their output state. Experimentally, χ is obtained by performing *quantum process tomography* (QPT) [11, 12]. QPT has been performed in a limited number of systems. A one-qubit teleportation circuit[13], and a controlled-NOT process acting on a highly mixed two-qubit state [14] have been investigated in liquid-state NMR. In optical systems, where pure qubit states are readily prepared, one-qubit processes have been investigated by both ancilla-assisted [15, 16] and standard [17] QPT. Two-qubit optical QPT has been prototyped by the investigation of a beamsplitter acting as a Bell-state filter [18].

We fully characterize a two-qubit entangling gate – a CNOT gate acting on pure input states – by QPT, maximum-likelihood reconstruction, and analysis of the resulting process matrix. In doing so, we address a significant problem in QPT experiments: that the naïve matrix inversion procedure in QPT, when performed on real (i.e., inherently noisy) experimental data, typically leads to an unphysical process matrix. Using our physical process matrix, we can accurately determine the action of the gate on any arbitrary input state, including the amount of mixture added and the change in entanglement. We also evaluate useful measures of gate performance.

The CNOT gate we characterize, in which two qubits are encoded in the polarization of two single photons, is a nondeterministic gate operating in the coincidence basis [19, 20]. The gate is known to have failed whenever one photon is not detected at each of the two gate outputs, and we postselect against these failure modes. This gate, described in detail in Ref. [20], produces output states that have high fidelity with the ideal CNOT outputs, including highly entangled states.

The idea of QPT [1, 11, 12] is to characterize a completely positive map $\mathcal{E}$, which represents the process acting on an arbitrary input state ρ:

$$\mathcal{E}(\rho) = \sum_{m,n=0}^{d^2-1} \chi_{mn} \; \hat{A}_m \rho \hat{A}_n^\dagger, \qquad (1)$$

where the $\hat{A}_m$ are a basis for operators acting on ρ. The matrix χ completely and uniquely describes the process $\mathcal{E}$, and can be reconstructed from experimental tomo-

graphic measurements. One performs a set of measurements (quantum state tomography [21], in fact) on the output of an n-qubit quantum gate, for each of a set of inputs. The input states and measurement projectors must each form a basis for the set of n-qubit density matrices, requiring $d^2 = 2^{2n}$ elements in each set [1, 22]. For a two-qubit gate ($d^2 = 16$), this requires 256 different settings of input states and measurement projectors. An alternative is *ancilla assisted process tomography* [15, 16], where a suitable single state of dimension $\geq d^2$ replaces the d^2 separable inputs.

The fact that standard QPT reconstruction techniques typically lead to an unphysical process matrix is a significant problem, as the predictive power of the process matrix is questionable if it predicts unphysical gate output states. However, the tomographic data can be used to obtain a *physical* process matrix by finding a positive, Hermitian matrix $\tilde{\chi}$ that is the closest fit in a least-squares sense, i.e. by finding a $\tilde{\chi}$ that minimizes the function

$$f(\vec{t}) = \sum_{a,b=1}^{d^2} \left(\frac{c_{ab}}{\mathcal{C}} - \sum_{m,n=0}^{d^2-1} \langle\psi_b|\hat{A}_m|\phi_a\rangle\langle\phi_a|\hat{A}_n|\psi_b\rangle\tilde{\chi}_{mn}(\vec{t}) \right)^2,$$
(2)

where $|\phi_a\rangle$ is the ath input state, $|\psi_b\rangle$ is the bth measurement analyzer setting, c_{ab} is the measured number of coincident counts for the ath input and b^{th} analyzer setting, $\mathcal{C}$ is the total number of coincident photon pairs within the counting time, and $\vec{t}$ represents a parametrization of $\tilde{\chi}$. The first term in the parentheses is the experimental measurement probability for a particular combination of settings; the second is the probability predicted from the process matrix. The technique is not architecture-dependent – the photon counts can be replaced with the relevant measurement probabilities for any realization of a two- (or more) qubit gate. This method parallels the maximum-likelihood technique for quantum state tomography [21]. A further set of constraints [1] is required to make sure that the matrix $\tilde{\chi}$ represents a trace-preserving process [24]: $\sum_{mn} \tilde{\chi}_{mn}\hat{A}_n^\dagger\hat{A}_m = I$. Using our CNOT data, we applied a global numerical minimization technique to find the minimum of $f(\vec{t})$, subject to these constraints (an alternative maximum-likelihood procedure was given in [23]).

In the Pauli basis, the ideal CNOT (a unitary operator) can be written as a coherent sum: $\hat{U}_{\text{CNOT}} = \frac{1}{2}(I \otimes I + I \otimes X + Z \otimes I - Z \otimes X)$; where the terms are tensor products of Pauli operators $\{I, X, Y, Z\}$ acting on control and target qubits respectively. The Pauli basis representation of the ideal CNOT, and our experimental process, are shown in Fig. 1(a)&(b). Physically, the process matrix shows the populations of, and coherences between, the basis operators making up the gate function (note the sign of the coherences corresponds to the

sign of the terms in $\hat{U}_{\text{CNOT}}$), analogous to the interpretation of density matrix elements as populations of, and coherences between, basis quantum states. In fact, process matrices are isomorphic with density matrices in a higher dimensional Hilbert space [25, 26], except that the trace-preservation condition constrains physical process matrices to a subspace of physical state density matrices.

It is important to consider how well the matrix $\tilde{\chi}$ describes the raw data. Clearly there will be some discrepancy, as the simple matrix inversion of the data (i.e. without maximum-likelihood estimation) produces an unphysical process matrix. It is possible to obtain some information about the confidence of the fit by examining the *residuals* (Fig. 1(c)), i.e. the differences Δ between each of the 256 measurement probabilities and the corresponding probabilities predicted from $\tilde{\chi}$. The width of this distribution, $\sigma(\Delta) = 0.026$, gives an idea of the relative error in the process tomography. Since the process matrix contains full information about the process, it can be used to predict the output state for any given input. We can further test the maximum-likelihood technique by comparing the predicted output state (as calculated from $\tilde{\chi}$) with the *experimentally determined* output density matrices for all 16 different inputs and find that the average fidelity and standard deviation between the predicted and measured density matrices are 0.95 and 0.03 respectively. This ability to predict accurately the outputs of the gate, for any input, is a key motivation for generating a maximum-likelihood *physical* process matrix.

Ultimately, we want to characterize the process relative to some ideal: in this case, χ_{CNOT}, which is the process matrix representing $\hat{U}_{\text{CNOT}}$. We use the *process fidelity* [26], $F_P = \text{Tr}(\chi_{\text{ideal}}\,\tilde{\chi})$, and find $F_P = 0.76$. We can obtain a graphical representation of the F_P by expressing the process matrix in the "CNOT" basis (obtained by multiplying all Pauli basis elements by $\hat{U}_{\text{CNOT}}$). In this case, F_P is simply the height of the corner (00) element, as shown in Fig. 1(d), and is an example of the insight that can be obtained by examining the process matrix in different bases. Currently, we are not able to put an error bar on F_P when it is calculated from $\tilde{\chi}$, because no technique is known for obtaining error estimates on the elements of $\tilde{\chi}$ (or the quantities derived from them), owing to the numerical minimization in the maximum-likelihood reconstruction procedure.

The fact that the fidelity of the process is given by the height of one element of $\tilde{\chi}$ in the CNOT basis suggests that F_P might be obtained with far fewer experimental settings than for full QPT. Indeed, we have found this to be true, even for separable input states and local measurements. In principle, only d^2 parameters are required to find F_P. For our (physically achievable) settings [22], the process fidelity with the ideal CNOT can be related directly to a 65-element subset of the tomographic data. Importantly, any such "direct" relationships also allow
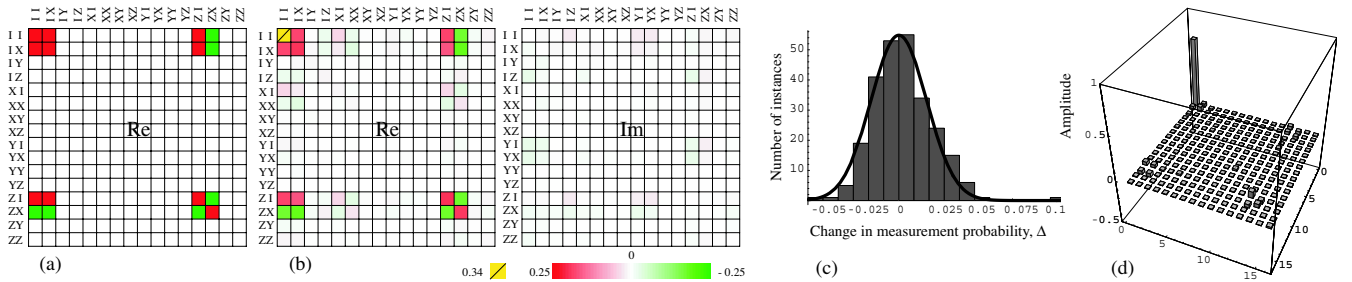
FIG. 1: Process matrix of the CNOT gate. (a) Ideal process matrix in the basis defined by tensor products of Pauli operators. (Imaginary part is identically zero). The *population* of each basis operator can be seen on the diagonal, and the *coherences* between operations can be seen in the off-diagonal elements. (b) Experimental realization determined by our maximum-likelihood QPT technique. (c) Histogram of the differences in probability between the experimental data and the maximum-likelihood reconstruction for the 256 tomographic measurements. The Gaussian fit $\gamma \exp(-x^2/\sigma^2)$ has $\sigma = 0.026$. (d) Real part of the experimentally determined process matrix, expressed in the CNOT operator basis, where the 00 element represents the component of U_{CNOT} in the process. The imaginary components of the elements are negligible, except for one coherence of magnitude 0.10. In this basis, an ideal CNOT gate has a value of unity for the 00 element; all other elements are zero. The abscissae are the abscissae of (a) and (b), multiplied by $\hat{U}_{\mathrm{CNOT}}$.

straightforward error estimates. Using this alternative technique, we find $F_P' = 0.82 \pm 0.01$ [29]. The error bars are small relative to the difference between F_P' and F_P, however, the error in F_P is not presently known, and may be significantly larger due to either the larger number of parameters involved in the estimate, or the minimization, or both.

The *average gate fidelity* $\overline{F}$ [30] is defined as the state fidelity [31] between the output of the gate and the ideal output, averaged over all input states. There is a simple relationship between the process fidelity and the average fidelity for any process [26], which we apply to our experimental values: $\overline{F}' = (dF_P' + 1)/(d+1) = 0.86 \pm 0.01$. We believe that the sub-unit fidelity primarily arises from imperfect mode matching (spatial and spectral overlap of the optical beams). In our gate circuit [20], imperfect mode matching results in imperfect nonclassical interference between control and target photons, and mixture of the individual qubit states as well. We find good correlation between the amount of mode mismatch and the measured fidelities. It is important to note that mode mismatch is not a fundamental limitation for optical quantum gates, and guided mode implementations promise an elegant solution.

Although the fidelity may seem like a simple method for comparing processes, it is not ideal, because it does not satisfy many of the requirements for a good measure. A full list of the desirable properties can be found elsewhere (e.g. Ref. [26]), but to some extent they can be summarized by the concept that an ideal measure must remain valid when used to characterize a gate as part of a larger quantum circuit, as well as in isolation. To this end, a new measure, the *process angle*, has been developed [26]: $A_P = \frac{2}{\pi} \arccos\left(\sqrt{F_P'}\right) = 0.28 \pm 0.01$. Although monotonically related to the process fidelity, it has all the properties required. The process angle is a

metric, so that two processes that are identical will have $A_P = 0$ (and orthogonal processes have $A_P = 1$) [32].

As well as the process fidelity (and related measures), it is important to quantify how much entanglement a gate generates, and how much mixture it introduces. We introduce a simple relation to characterize the latter (for details, see[26]): $\overline{\mathrm{Tr}\left(\rho^2\right)} = (d\,\mathrm{Tr}(\tilde{\chi}^2) + 1)/(d+1) = 0.71$, where the quantity on the left hand side is the purity of gate output states, averaged over all pure inputs. This corresponds to an average normalized linear entropy [33] of 0.39.
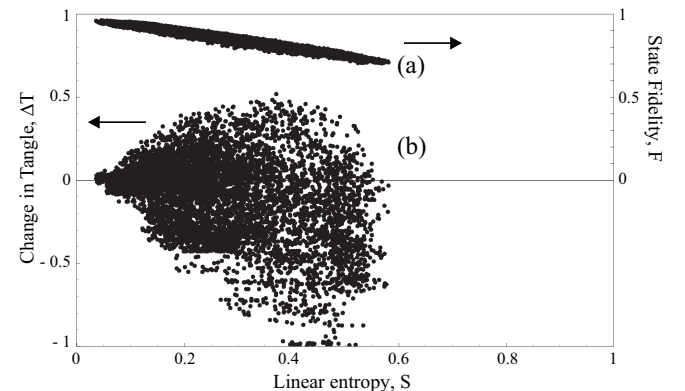

FIG. 2: (a) State fidelity of our CNOT gate outputs (with ideal CNOT output states) calculated from $\tilde{\chi}$, plotted against the linear entropy added by the gate. A perfect experimental CNOT process would have F=1, S=0 for all states. (b) Change in tangle between input and output, and linear entropy added, for our CNOT gate outputs, calculated from $\tilde{\chi}$. An ideal CNOT would have points distributed between -1 and 1 on the y axis, and S=0. For both plots, the gate inputs were ~189000 pure states uniformly distributed in the state space.

An instructive method for examining the action of the

gate, in terms of fidelity, entanglement and entropy, is to make scatter plots of these quantities for output states of the gate (Fig. 2). We used $\sim$189000 pure, uniformly distributed input states, and the $\tilde{\chi}$ matrix, to predict a distribution of output states of our experimental gate. From this data, we can observe the effect of mixture on the entanglement generated by the gate, and on the gate output state fidelity. The gate has three separate spatial mode matching conditions [20], and the contribution of each of these to the overall mixture is state dependent, leading to the distribution of entropies. There is a clear correlation between the fidelity and the amount of mixture added, showing that the mixing process is the dominant cause of gate imperfection – the gate occasionally fails because it mixes the states, not because it sometimes coherently performs the wrong operation. The scatter plot reveals that the minimum output state fidelity is 0.69. The shape of the upper lobe ($\Delta T > 0$) of the ΔT vs. S plot (Fig. 2(b)) is readily understood by the state-dependent mode matching considerations. States that have the largest change in tangle correspond to cases when the gate requires all three mode matching conditions to be simultaneously satisfied, and since each is not perfectly satisfied, this introduces a large amount of mixture. When only one mode matching condition applies, the gate cannot perform an entangling operation, but only a little mixture is added. The extension of the lower lobe ($\Delta T < 0$) to $\Delta T = -1$ (asymmetric with the upper lobe) can be explained by the fact that when the gate acts to disentangle the input, the addition of mixture also reduces the tangle. We find that the maximum increase in tangle of the gate (the entangling capability [12]) is $\Delta T_{\max} = 0.54$. This value is smaller than the largest tangle ($T = 0.65 \pm 0.06$) that we observed in an earlier experimental investigation [20]. This discrepancy is not unexpected, in that the tangle is known to be a harsh measure – small changes in the fidelity of a given state with a maximally-entangled state can lead to large changes in the tangle [34]. Using a different measure of entangling potential – the maximum fidelity of the output state (for separable inputs) with a maximally entangled state – yields 0.84 for the present data and 0.88 for the data in Ref. [20].

In summary, we have demonstrated the full characterization of a two-qubit entangling quantum process – a controlled-NOT gate acting on arbitrary inputs – by applying *physical* quantum process tomography. With the process matrix, we can predict, with approximately 95% fidelity, the action of the gate on an arbitrary two-qubit input state. We determine: an average gate fidelity of 0.81 using the process matrix, and 0.86 ± 0.01 using a set of 65 input and measurement settings; an average gate purity of 0.71; a process angle of 0.28 ± 0.01; and a maximum increase in tangle of 0.54. The main failure mechanism of the gate can be observed from the process matrix in the Pauli basis, and the scatter plots – some of

the operator population is incoherently redistributed so that the gate performs the identity operation with higher probability than for the ideal CNOT, a mechanism that we assign primarily to the imperfect mode matching of the interferometers. Process matrices such as these can be used to predict the action of real-world gates in quantum circuits.

* URL: www.quantinfo.org
[1] M.A. Nielsen and I.L. Chuang, *Quantum Computation and Quantum Information* (Cambridge University Press, Cambridge, 2000).
[2] N. Gisin, *et al.*, Rev. Mod. Phys. **74**, 145 (2002).
[3] J.P. Dowling and G.J. Milburn, Philos. Trans. R. Soc. London, Ser. A **361**, 1655 (2003).
[4] J.L. Brylinski and R. Brylinski, in *Mathematics of Quantum Computation*, edited by R.K. Brylinski and G. Chen (Chapman and Hall/ CRC Press, Boca Raton, 2002).
[5] E. Knill, R. Laflamme, and G.J. Milburn, Nature **409**, 46 (2001).
[6] T.B. Pittman, B.C. Jacobs, and J.D. Franson, Phys. Rev. A **64**, 062311 (2001).
[7] M. Koashi, T. Yamamoto, and N. Imoto, Phys. Rev. A **63**, 030301 (2001).
[8] G.J. Pryde, *et al.*, quant-ph/0312048 (2003).
[9] P. Kok, H. Lee, and J.P. Dowling, Phys. Rev. A **66**, 063814 (2002).
[10] G.J. Pryde and A.G. White, Phys. Rev. A **68**, 052315 (2003).
[11] I.L. Chuang and M.A. Nielsen, J. Mod. Opt. **44**, 2455 (1997).
[12] J.F. Poyatos, J.I. Cirac, and P. Zoller, Phys. Rev. Lett. **78**, 390 (1997).
[13] M.A. Nielsen, E. Knill, and R. Laflamme, Nature **396**, 52 (1998).
[14] A.M. Childs, I.L. Chuang, and D.W. Leung, Phys. Rev. A **64**, 012314 (2001).
[15] J.B. Altepeter, *et al.*, Phys. Rev. Lett. **90**, 193601 (2003).
[16] F. De Martini, *et al.*, Phys. Rev. A **67**, 062307 (2003).
[17] Y. Nambu, *et al.*, Proc. SPIE **4917**, 13 (2002).
[18] M.W. Mitchell, *et al.*, Phys. Rev. Lett. **91**, 120402 (2003).
[19] T.C. Ralph, *et al.*, Phys. Rev. A **65**, 062324 (2002).
[20] J.L. O'Brien, *et al.*, Nature **426**, 264 (2003).
[21] D. F. V. James, *et al.*, Phys. Rev. A **64**, 052312 (2001).
[22] We use polarization to encode the state of our qubits, with $|H\rangle = |0\rangle$ and $|V\rangle = |1\rangle$. Then $\sqrt{2}\,|D(A)\rangle = |H\rangle + (-)|V\rangle$ and $\sqrt{2}\,|L(R)\rangle = |H\rangle + (-)i|V\rangle$. The input states

|Control Target⟩ are taken from {HH, HV, DV, RH, RV, VV, HV, HA, HR, RR, RA, DA, DL, VA, VR, DH} and the measurements ⟨CT| from {HH, HV, VH, VV, HD, HL, VL, VD, DD, RL, RD, DR, DV, RV, DH, RH}.

[23] M. Ježek, J. Fiurášek, and Z. Hradil, Phys. Rev. A **68**, 012305 (2003).

[24] The postselective nature of our experiments precludes maps that are not trace-preserving (e.g., where one or more photons are lost).

[25] A. Jamiolkowski, Rep. Math. Phys. **3**, 275 (1972).

[26] A. Gilchrist, N.K. Langford, and M.A. Nielsen, University of Queensland preprint (2003).

[27] M. Barbieri, *et al.*, Phys. Rev. Lett. **91**, 227901 (2003).

[28] A.G. White, *et al.*, quant-ph/0308115 (2003).

[29] These error bars are calculated from Poissonian photon counting statistics.

[30] M.A. Nielsen, quant-ph/0205035 (2002).

[31] We use $F_{\text{state}} = \left(\text{Tr}\sqrt{\sqrt{\rho}\,\sigma\,\sqrt{\rho}}\right)^2$ to calculate the fidelity between states represented by density matrices ρ and σ.

[32] A related metric is the *process distance* D_P [26], which uses the isomorphism between states and processes to calculate the equivalent of a state trace distance [1]. $D_P = 0$ for an ideal gate; we find $D_P = 0.29$ for our gate.

[33] W.K. Wootters, Phys. Rev. Lett. **80**, 2245 (1998); A.G. White, *et al.*, Phys. Rev. A **65**, 012301 (2001).

[34] N.A. Peters, *et al.*, quant-ph/0308003 (2003).